Investigation spatial distribution of droplets and the percentage of surface coverage during dropwise condensation

Solmaz Boroomandi Barati, Nicolas Pionnier, Jean-Charles Pinoli, Stéphane Valette, Yann Gavet

Investigation spatial distribution of droplets and the percentage of surface coverage during dropwise condensation

S. Boroomandi Barati*[1], N. Pionnier[2], J.-C. Pinoli[3], S. Valette[2], and Y. Gavet[3]

[1]Univ Lyon, Ecole Nationale Supérieure des Mines de Saint-Etienne, LGF UMR CNRS 5307, SAINT-ETIENNE, France
solmaz.boroomandi@emse.fr
[2]Univ Lyon, Ecole Centrale de Lyon, LTDS UMR CNRS 5513, F-69134, LYON, France
[3]Ecole Nationale Supérieure des Mines de Saint-Etienne, LGF UMR CNRS 5307, SAINT-ETIENNE, France

Abstract

The aim of this research is to develop an algorithm to simulate droplets nucleation and growth during dropwise condensation in order to study the droplets spatial distribution. The proposed algorithm starts with droplets distributed based on the Poisson point process and investigates the spatial distribution of droplets using Ripley's L function method. Also, the effects of substrate temperature (T_w) and initial density (N_D) on the percentage of area occupied by droplets (ϕ) are studied. Good agreement between model predictions and experimental data for the rate of growth and changes in droplets density (N_t) as well as spatial distribution of droplets verifies the validity of the simulating model.

Keywords: Dropwise condensation, Ripley function, Poisson point process, Percentage of surface coverage

1 Introduction

The process of dropwise condensation attracted lots of attention since about 80 years ago, when Schmidt et al. [1] proved that it's heat transfer coefficient is significantly higher than filmwise condensation. Filmwise condensation refers to the process in which the surface of substrate is covered by a film of liquid, while dropwise condensation happens when the contact angle of liquid on the surface is not low enough to form a stable liquid film [2]. This definition bears in mind the concept of Cassie–type and Wenzel-type droplets. Cassie droplets sit on top of the textured surface with trapped air underneath, whereas Wenzel droplets retain intimate contact with the solid surface [3]. Depending on the goal of process, each of these types can be more favored. Cassie droplets which lead to dropwise condensation are preferred when higher rate of heat transfer is needed, for example in heat exchangers or when an easy-to-clean surface aims to reduces pollutant adhesiveness [4]. This process has a great importance in analyzing and manufacturing condensers, heat exchangers and other steam operating devices. The problem that we are dealing with is the formation of liquid droplets in car light shield which will cause the light reflection and as a result

*corresponding author

the decrease in the efficiency of illumination. In such cases it is preferred to achieve the Wenzel droplets and even filmwise regime.

The first attempts to numerically simulate dropwise condensation were done by presenting a model thorough which, nucleation of small droplets, adsorption and coalescence occur iteratively. There were some weaknesses in this algorithm, for example the algorithm started based on monodispersity of initial configuration of droplets meaning that all the initial droplets had the same size [5], or the growth rate was calculated considering just the effect of heat convection through a droplet [6], also in some other articles the center point of droplets after coalescence was considered in the center of bigger droplet [7]. This classic model was modified step by step, but still has inaccuracy in some details. For example, the spatial distribution of droplets was not studied. Spatial distribution deals with the position of droplets on the substrate that can affect the coalescence procedure. Also, the size distribution of new nucleations was not considered in these studies.

Rose was one of the first scientists who carried out a considerable amount of studies on the dropwise condensation. Le Fevre and Rose [8] modeled condensation heat transfer, considering the effect of surface tension, conduction thorough droplets, and dissipation associated with mass transfer for droplets that are not big enough to sweep the surface. In the following research, Rose [9] developed the same heat transfer equation for the falling drops also. To investigate time-average features of the size distribution and the percentage of surface occupied by droplets, Tanaka [10] numerically solved two equations relating to the spatial distribution of droplets . According to him [11, 10], dropwise condensation is closely influenced by three dynamic characteristics: (1) drop-size distribution density, (2) substantial growth rate of drops by condensation, and (3) growth rate of drops by both condensation and coalescence. Rose and Glicksman [12] derived a power law model to describe the first parameter that is drop-size distribution density. Mei et al. derived a time-average fractal model based on fractal geometry theory [13]. The importance of their work is due to describing drop size distribution function by parameters that have physical meanings, such as surface fraction, fractal dimension, and the maximum radius of droplets.

More recently, continuing the attempts to derive a model describing evolution of the droplets density (N_t) during time, Vemuri and Kim [14] developed their model using the population balance concept to predict the drop-size distribution of small drops which mainly grow by direct condensation. Tianyi et al. [15] presented a clustering physical model to describe the state of steam molecules before condensing on the cold substrate that affects droplets size distribution. El-Adawia and Felemban [16] suggested a statistical model to study the distribution of droplets size. Recently, Liu and Cheng [17] developed an improved thermodynamic model to describe dropwise condensation in all contact angles and considered the effects of coating thermal resistance as well as coating thermal conductivity. They then used this thermodynamic model to study the effect of four parameters including degree of subcooling, which is the difference between air saturated temperature and wall temperature $\Delta T_{sub} = T_{sat} - T_w$, contact angle, coating thickness, and thermal conductivity of coating on N_t [18]. Stylianou and Rose [19] discussed different methods to describe transition mode from dropwise to filmwise condensation like, viscosity-limited coalescence mechanism or nucleation site saturation mechanism.

The goal of the present study is to simulate dropwise condensation using a model based on physical fundamentals of this process. Then the results of this model is used to study the effect of wall temperature (T_w) and initial nucleation site density (N_D) on the area occupied by the droplets (ϕ). The higher percentage of area occupied by uniform and big droplets will lead to less light reflection through illuminating devices in humid days.

This model is modified in some details with respect to already-existing models.

- In this model spatial distribution of droplets from first configuration to steady state step is taken into account by studying Ripley's L function at each step. Steady state here means the time at which temporal changes are negligible .

- Based on the Ripley's L function of initial droplets, the algorithm starts by distributing

first droplets completely randomly according to the Poisson point process model.

- The probability density function is used to study the number and size of droplets nucleate at each step.

2 Physical aspect of dropwise condensation

In the process of dropwise condensation, at first small droplets nucleate all around the surface. Then, these small droplets start to grow by adsorbing water molecules from humid air. After a while if two or more droplets become big enough to overlap, they will merge and form a bigger droplet -called daughter droplet- in the mass center of the parents [20]. This phenomenon is called coalescence in literature. Although coalescence is a mass conservative process, the area covered by daughter droplet is lower than the summation of area covered by it's parents. This will lead to forming vacant area around daughter droplet, in which new small droplets can nucleate and grow. Both these steps will change N_t during time and lead to a temporal distribution [21]. Finally, the big droplets that can not resist the gravity force will slide and produce more vacant area on the surface. Therefore five main steps can be considered in a process of dropwise condensation: initial nucleation, growth due to adsorption, growth due to coalescence, nucleation of new small droplets, and departure of big droplets.

2.1 Initial nucleation

Nucleation refers to the process of forming a new thermodynamic phase from a bulk phase that can occur homogeneously or heterogeneously [15]. In dropwise condensation on the surface, nucleation means formation of small droplets that are ready to grow. If these droplets form on a completely flat surface with no preference, it will be an homogeneous nucleation. An heterogeneous nucleation occurs when there are some points due to pollutants or surface topography that are more potential to grow droplets. Most of the time, by considering the assumption of flatness, droplets nucleation is taken into account as homogeneous nucleation [22, 23]. So, it is possible to consider the distribution of initial droplets on the flat surfaces as a completely random distribution known as Poisson point process that has three main assumptions

1) The probability of detecting more than one droplet in a given interval δm is vanishingly small for sufficiently small δm (m can be volume or space).

2) Drop counts in non-overlapping intervals are statistically independent random variables (at any length scale) meaning that the probability of finding a droplet in each interval is independent of having a droplet in another intervals.

3) The process is statistically homogeneous which means that the mean and variance of random variable are constant along the domain of observation [24].

Figure 1 represents the Ripley function of initial configuration of droplets compared to the Poisson point process. Ripley function counts the number of points in specified distances from center of substrate and can be a useful method to study the spatial distribution of any event. This method can be formulated in two ways, Ripley's K function, that calculates events distribution according to equation 1 and Ripley's L function, that is the linerized form[25].

$$\hat{K}(x) = \hat{\lambda}^{-1} \sum_{i} \sum_{j \neq i} w(l_i, l_j)^{-1} \frac{I(d_{ij} < x)}{N}, \tag{1}$$

where d_{ij} is the distance between the ith and jth points, and $I(x)$ is the indicator function with the value of 1 if x is true and 0 otherwise. However, since the boundaries of the study area are usually arbitrary, edge effects arise because the points outside the boundary are not counted in the numerator, even if they are within the distance x of a point in the study area. The weight function, $w(l_i, l_j)$, provides the edge correction. It has the value of 1 when the circle centered at l_i and passing through the point l_j (i.e. with a radius of d_{ij}) is completely inside the study area.

If part of the circle falls outside the study area (i.e. if d_{ij} is larger than the distance from l to at least one boundary), then $w(l_i, l_j)$ is the proportion of the circumference of that circle that falls in the study area. The effects of edge corrections are more important for large x because large circles are more likely to be outside the study area [25].

In practice in it is easier to use linear form of Ripley's K function ($\hat{L}(x) = \sqrt{\frac{\hat{K}(x)}{\pi}}$) that is so called Ripley's L Function [25]. For a completely randomly distribution or Poisson point process Ripley's L function is a straight line passing from the points (0,0) and (100,100). The acceptable accordance between spatial distribution of initial droplets and Poisson point process that is shown in figure 1 indicates that initial droplets distribute randomly on a flat surface.

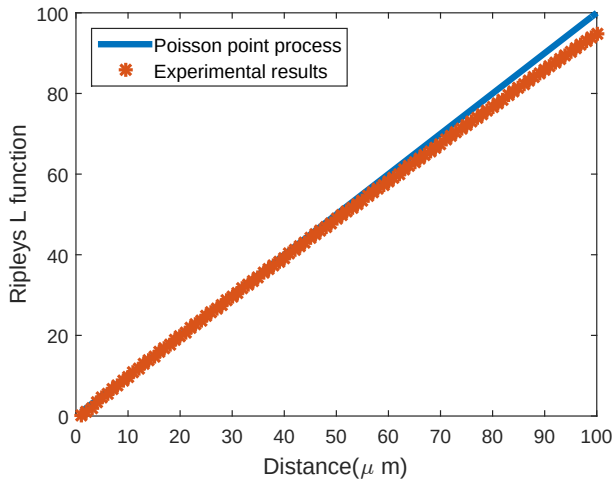

Figure 1: Ripley's L function of initial droplets distribution

2.1.1 Droplets arrangement

It is worth to point out here that the arrangement of droplets on the surface plays a very important role in controlling the rate of growth of droplets in the dropwise condensation on solid substrate. Configuration of droplets on the surface will change the possibility of contact between droplets and as well, the rate of growth due to coalescence, and consequently the rate of producing vacant area after coalescence that will change the number of new small droplets nucleate at each step. The arrangement of droplets is in close relationship with surface wettability and roughness. Therefore, one of the ways to change droplets arrangement is to apply chemical coatings that can change surface wettability, or to make different topographies on the surface to arrange the places that are more preferred to grow droplets. Both of these parameters will affect the number of droplets that are able to grow on the surface. Thus, studying the effect of different values for initial nucleation site densities on the growth rate of droplets seems also an interesting goal of each simulation procedure.

2.2 Adsorption

As it is said before, the first step in dropwise condensation is nucleation of small droplets that is randomly on the flat surface. Lots of droplets with variable sizes can form in this step but just the ones with radius bigger than a minimum value can grow and the rest will evaporate and disappear. r_{min} is the minimum size for droplets that are able to grow and the droplets smaller than this radius are assumed to disappear [26, 5].

$$r_{min} = \frac{2\sigma T_{dew}}{H_{fg}\rho(\Delta T_t)}. \tag{2}$$

In this equation, σ is water surface tension, H_{fg} is the latent heat of condensation, ρ is water density, T_{dew} represents dew point of humid air and ΔT_t is total temperature gradient that is the main driving force for adsorption. ΔT_t is equal to wall temperature and T_{dew} gradient ($\Delta T_{w-dew} = T_w - T_{dew}$) minus temperature gradient due to surface curvature (ΔT_{CD}):

$$\Delta T_t = \Delta T_{w-dew} - \Delta T_{CD}, \tag{3}$$

ΔT_{CD} is the temperature difference due to droplet's curvature, which is the temperature drop of a curved surface with respect to a planar surface. This temperature difference can be calculated by equation 4:

$$\Delta T_{CD} = \frac{2\sigma T_{dew}}{H_{fg}\rho r}, \tag{4}$$

where r represents the radius of droplets. Total heat transfer is equal to ΔT_t divided by summation of heat resistances between hot air and cold substrate including conductivity resistance between droplet and its surroundings and conduction thorough the droplet itself [27]:

$$R = \frac{1}{2\pi r^2 h_i(1 - Cos\theta_a)} + \frac{\theta_a}{4K_w \pi r Sin\theta_a}, \tag{5}$$

where K_w is water thermal conductivity, θ_a advancing contact angle, and h_i is the interfacial heat transfer coefficient which can be calculated from:

$$h_i = \frac{(2\alpha)}{(2-\alpha)} \sqrt{(M/(2\pi \dot{R} T_{dew}))} \frac{(H_{fg}^2)}{(T_{dew} v_g)}. \tag{6}$$

v_g here is specific volume of gas phase, M is molecular weight of water and $\dot{R}$ is the gas universal constant. α is the condensation coefficient related to non-condensible gases mixed with air. In the absence of non-condensible gas $\alpha = 1$. Combining equations 3 to 6 the total heat transfer can be calculated as

$$q = \frac{\Delta T_{sat-wall} - \frac{2T_{dew}\sigma}{H_{fg}\rho r}}{\frac{1}{2\pi r^2 h_i(1-Cos\theta_a)} + \frac{\theta_a}{4K_w \pi r Sin\theta_a}}. \tag{7}$$

On the other hand, heat of condensation is equal to the mass of condensate multiple by the latent heat of condensation:

$$q = \rho_l H_{fg} \pi r^2 (1 - Cos\theta)^2 (2 + Cos\theta) \frac{dr}{dt}. \tag{8}$$

By equaling equations 7 and 8, the size of droplets of next generation can be calculated according to Euler method in solving ordinary differential equations:

$$r_k = r_{k-1} + G, \quad G = \frac{dr}{dt} = \frac{C_1(1 - \frac{r_{min}}{r})}{C_2 + C_3 r} \tag{9}$$

where k represents each generation of droplets and $C_1 = \frac{1}{(1-Cos\theta)^2(2+Cos\theta)} \frac{\Delta T_{sw}}{\rho H_{fg}}$, $C_2 = \frac{1}{2h_i(1-Cos\theta_a)}$, and $C_3 = \frac{\theta_a}{4K_w Sin\theta_a}$.

2.3 Coalescence

The droplets grow continuously with the rate of G according to equation 9. When two droplets (the so-called parents) become big enough to touch, they will merge and form a bigger one named daughter drop. This means that if the Euclidean distance between two droplets ($L_{i,j}$) with sizes r_i and r_j becomes less than $r_i + r_j$ they will coalesce and form a bigger droplet in the mass center of the original drops with size r that is given by:

$$r = \sqrt[D]{r_i^D + r_j^D}, \tag{10}$$

where D is the droplets dimension. $L_{i,j}$ is the Euclidean distance between two droplets center. For $d = 2$, $L_{i,j}$ is:

$$L_{i,j} = \sqrt{(x_i - x_j)^2 + (y_i - y_j)^2} : \tag{11}$$

and for $d = 3$ is:

$$L_{i,j} = \sqrt{(x_i - x_j)^2 + (y_i - y_j)^2 + (z_i - z_j)^2}. \tag{12}$$

Coalescence is generally described by the dimension of drops (D) and dimension of substrate (d) while $D \geq d$ [28]. D and d must be determined by the process, for example in the formation of dew on the cobweb three dimensional drops form on one dimensional thread. In this case $d = 1$ and $D = 3$ or in the case of formation of hemispheric droplets on the plate $d = 2$ and $D = 3$ as well. It is worth to point out here that there are two different situations depending on d and D [28].

1. If $D = d$: in such situation after a while a single droplet will form that can extent across the entire system. This is the concept of gelation or percolation. For example in the reaction of silans and water in acidic or basic solution, droplets of silan hydroxide grow in 3 dimension ($d = 3$ and $D = 3$) and after a while gelation occurs and the whole solution turns in to a unique droplet.

2. If $D > d$: in this case there is no gelation in a finite time and the process continues in the same manner as low-density colloidal aggregation, in which particles can merge but do not form a unique big particle. This is the case of dropwise condensation on the flat surface ($d = 2$ and $D = 3$). The droplets grow and coalesce but the whole system will never unite.

Some times coalescence is the combination of more than two droplets (multiple coalescence). This happens especially when two big droplet adsorb each other and there are some small droplets in the space between them. This effect can be seen in 2.

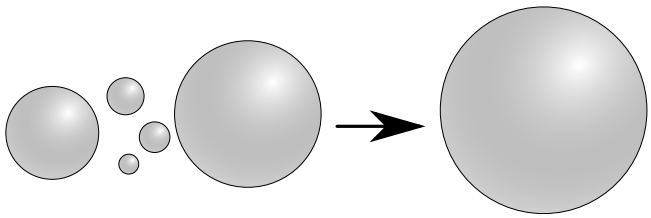

Figure 2: Multiple coalescence: two big droplets adsorb each other and swallow the small droplets in their between.

2.4 Nucleation of new droplets

As was mentioned before, nucleation of new drops in the vacant area produced during coalescence occurs continuously along the process. Number and size of new droplets can be calculated based on probability density function (PDF) of droplets during condensation process (figure 3). In this figure vertical axis represents the average droplets size at each step (r_{ave}). This figure shows that at first there is a unimodal distribution due to Poisson point process (see figure 1) with the peak concentrated on small droplets with size of 6 μm. The mean of PDF then will move towards bigger values due to droplets growth, and after a while another peak around small droplets will appear again. In this step, PDF will turn into a bimodal shape. The second peak relates to nucleation of new small droplets in the vacant area of substrate and stays on this point until the end of process.

This peak must present in the area near the size of initial small droplets, but since the image processing method eliminated very small droplets between the bigger ones, the second peak related to the average size of small droplets appears around $20\mu m$.

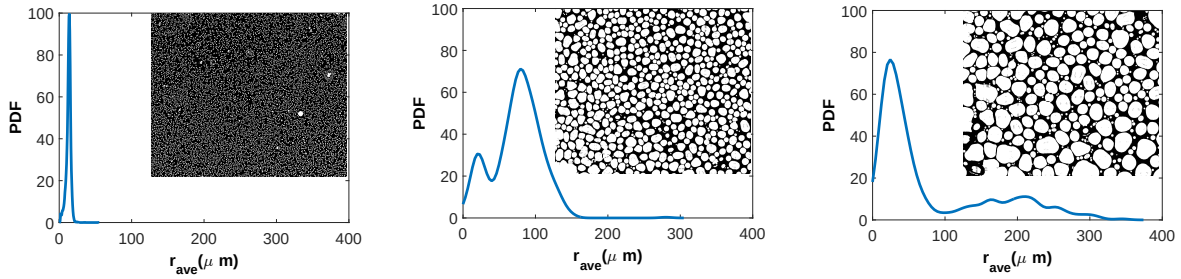

Figure 3: Probability density function (PDF) of number of droplets in each size range at three time steps: (a) $t = 200s$, (b) $t = 2500s$, (c) $t = 5000s$.

2.5 Departure of big droplets

The droplets continue growing until their weight becomes bigger than the adhesive force with the surface, that according to [29] comes from surface roughness and contact angle hysteresis. When droplets become heavy enough to overcome the adhesive force, they will slide and clean off the droplets that are in their path. The check for departure can be done by comparing the gravity force and adhesive force affecting to each droplet. The gravity force for a droplet with advancing and receding contact angles θ_a and θ_r is [30]:

$$F_g = (2 - 3Cos\theta_e + Cos^3\theta_e)\pi r_{max}^3 \rho_l g. \tag{13}$$

The adhesive force with the surface can be assumed as the surface tension force [31]:

$$F_\sigma = 2\sigma r_{max} Sin\theta_e (Cos\theta_r - Cos\theta_a). \tag{14}$$

θ_e here is the apparent equilibrium contact angle and is equal to $Cos^{-1}(0.5Cos\theta_a + 0.5Cos\theta_r)$. r_{max} that is the maximum radius of each generation of droplets before sliding can be calculated by equaling the equations (13) and (14) as [30]:

$$r_{max} = \sqrt{\frac{6(Cos\theta_r - Cos\theta_a)Sin\theta_e\sigma}{\pi(2 - 3Cos\theta_e + Cos^3\theta_e)\rho g}}, \tag{15}$$

where σ is liquid surface tension, ρ_l and ρ_v are liquid and vapor density respectively, and g is the earth acceleration.

2.6 Experimental apparatus

During experimental procedure, water droplets are formed on the poly carbonate surface of $3.27mm \times 2.7mm$ with temperature of around $17°C$ in contact with humid hot vapor. Vapor

temperature is set at $30°C$ with relative humidity of 40% that is maintained by compressor outside the chamber. High resolution CCD camera is used to record nucleation and growth of droplets in time interval of $1s$. Illustration of the set-up can be seen in figure 4.

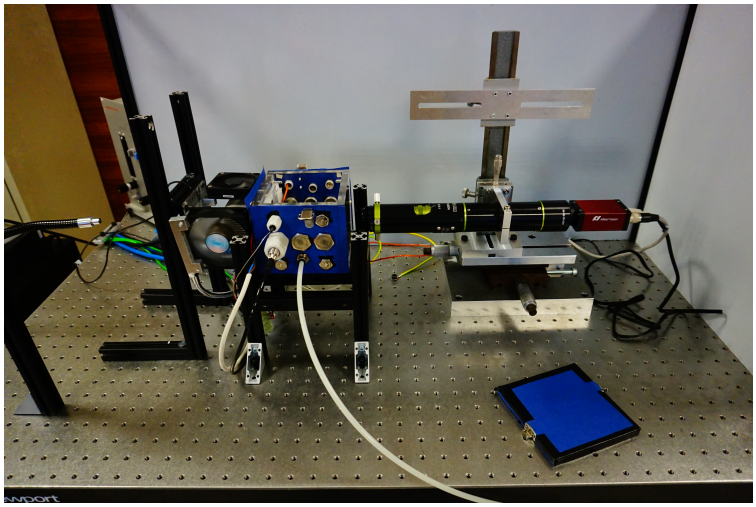

Figure 4: Illustration of the experimental set-up

The images taken by CCD camera then are binarized and used as the basis of the simulating model. These binarized images are presented in figure 5. In this figure different steps of dropwise condensation are marked, including initial nucleation, droplet growth due to adsorption, droplet growth due to coalescence, nucleation of new droplets, and departure of big droplets. These binarized images are used to extract information of droplets size, number and total area of droplets at each time step to validate the results of simulation. The initial information is as below:

Number of droplets= 13497, size range $6.7 \times 10^{-6} \pm 0.2 \times 10^{-6} m$, and area of substrate $9mm^2$.

3 Model for simulating droplets nucleation and growth

The present model is based on physical description of dropwise condensation. At first 13479 random droplets with density of $N_t = 1.29 \times 10^8 m^{-2}$ are distributed completely randomly according to the Poisson point process method. Each droplet then grows through a main loop which consists of three parts.

- Nucleation of new droplets: New small droplets with size and radius calculated according to method described in section 2.4 are added in each step. After addition of these new droplets their overlaps with already-existing droplets is checked in an inner loop.

  It is important to locate the new small droplets in the vacant area between already-existing droplets. We did this process inside an inner loop, during which the Euclidean distance between the new drops and already-existing droplets is calculated and if it is smaller than the radius of already-existing droplet, then they will coalesce and the small drop will be eliminated.

- Adsorption: In this part, all the droplets grow with the rate of G according to equation 9.

- Coalescence: It is worth to point out here that in order to take into account the multiple coalescence, after each coalescence the distance between daughter droplet with all the already-existing drops is checked in an inner loop and if one of the already-existing droplets is inside the area of the daughter drop they will merge.

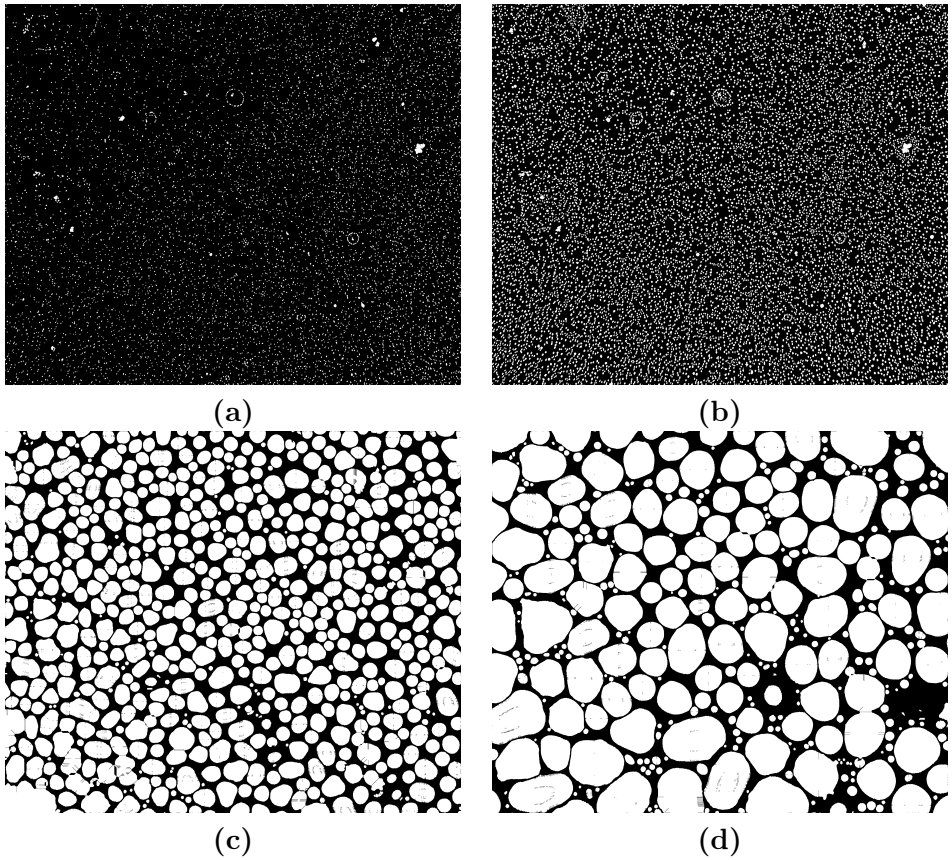

Figure 5: Binarized images of real droplets taken by CCD camera during experiments. These images are chosen in the main phases of droplets growth: (a) nucleation of small droplets, (b) growth due to adsorption, (c) growth due to coalescence, (d) nucleation of new small droplets.

- Departure of big droplets: At the end of each step there is a check for departure of big droplets that cannot resist against gravity force. These heavy droplets will slide and clean off other droplets in their path and reproduce more vacant area to grow new small droplets.

At the end of the main loop there is a check for steady state, meaning that the difference between the size of droplets at iteration k and the size of droplets at iteration $k-1$ is calculated. If the difference is smaller than a pre-specified error, then the loop will stop. Schematic diagram of simulation process is described in figure 6.

Choosing time step in this algorithm is very important, obviously the smaller time steps need considerable calculating time, on the other hand very big time steps will cause to the loss of some data regarding the droplets growth and nucleation of new small droplets. In this algorithm we choose time step of $10^{-4}s$ for calculating the growth rate due to adsorption in order to have more accurate answers of Euler method and we collect the information for comparing with experimental results at each $10s$. The program was written in matlab and was run on a 2 cores PC with Intel Xeon CPU E5-2630 (2.40GHz), with 20gb ram and it took around 3 hours till completing in around 500 steps.

The results of the program for five different T_w and four different N_D are compared with experimental results in order to investigate the effective parameters in controlling droplets growth in dropwise condensation.

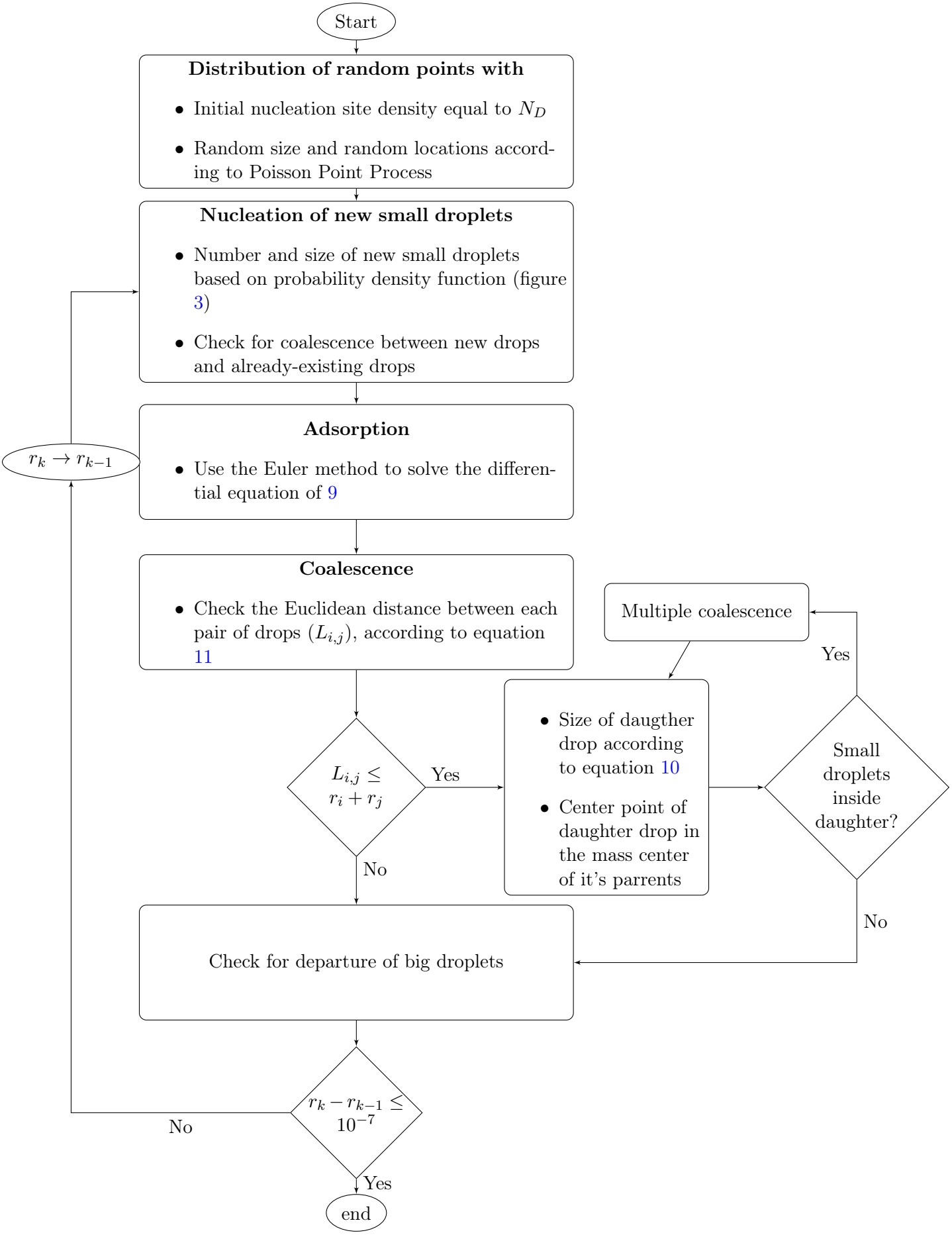

Figure 6: Schematic diagram of the simulation algorithm

4 Results and discussion

In this part at first, the validity of the simulating model will be verified by comparing it's results with experimental data. Then, the effect of T_w and N_D on the percentage of surface covered by water droplets will be discussed in the following parts.

4.1 Comparison between simulation results and experimental data

Comparison of N_t and r_{ave} between simulation results and experimental data are presented in figure 7. This figure shows acceptable accordance between these two parameters in simulation and experiments. According to this figure at first, droplets grow very rapidly due to adsorption, also coalescence and nucleation of new droplets accelerate the rate of growth which lead to a fast reduction in the number of droplets in earlier stages. After a while due to forming vacant area between droplets, the rate of coalescence reduces because the distance between droplets is larger with respect to the initial stages. On the other hand the, droplets are bigger and the friction factor with substrate resists against coalescence. In addition, very big droplets transfer lower heat flux between cold surface and hot vapor and as a result will decrease the rate of droplets growth [5]. Therefor in final stages there is higher amount of vacancies on the substrate that are ready to grow new small droplets and the rate of coalescence of already-existing droplets reduces. Steady state situation in these graphs comes from the opposite effects of coalescence and nucleation of new small droplets. Coalescence increases the size of droplets rapidly and reduces N_t, while nucleation of new droplets lowers r_{ave} and increases N_t. In [32] the term of steady is used in opposite of non-steady, in which millions of coalescence occur in a square of $1 \times 1cm^2$ at each second. On the other hand, Tanaka [10, 33] studied the photographs of a vertical condensing surface, and he stated that steady state achieved in dropwise condensation when the surface is cleared of condensate periodically by sliding big drops. These drops sweep the surface, exposing bare strips, on which transient condensation takes place without delay, until the area is swept clean again [34]. Based on these references and the definition that states steady state occurs when changes during time are negligible, we interpret steady state as the situation under which the droplets are big and surrounded by vacant area produced by coalescence and sliding of bigger droplets so they are not able to coalesce rapidly. On the other hand small droplets nucleate in these vacancies and the challenge between these two effects will cause a constant pattern in graphs of droplets radius and density and will lead to steady state situation. This will happen during sliding the big droplets.

It must be noticed here that, since the average contact angle for experimental droplets is 88° we assume that the droplets are hemispheres and perfectly circular. In the earlier stages the shape of droplets is circular but when droplets grow due to coalescence, the friction force between droplet and substrate makes it harder to slide on the surface and form the perfectly circular shape. Therefor, the small difference between graphs of experimental and simulation can be because of this effect.

Figure 8 illustrates the real droplets and droplets generated by the proposed model at three different time intervals ($t = 1s$, $t = 700s$, $t = 5000s$). It can be seen that the assumption of circular droplets is not far from reality specially in the earlier stages, but at steady state the droplets are very big and they cannot slide on the surface and form a perfectly circular shape.

It was explained that before steady state N_t changes rapidly, that will lead to change in spatial distribution of droplets. In this regard, Ripley's L function method which counts the number of drops in specified distances from center of substrate can be considered as a useful tool to evaluate simulation method (figure 9). It can be seen that there is a visible similarity between Ripley's L function of simulation results and experimental data. The blue straight line represents Ripley's L function of the Poisson point process dealing with completely randomly distributed points. Any positive and negative deviation from this line indicates dispersion and coalescence, respectively. In the Ripley's L function of both experimental and simulation results, a minimum distance of around 6 μm is appeared between droplets that is equal to the size of the smallest droplets exist

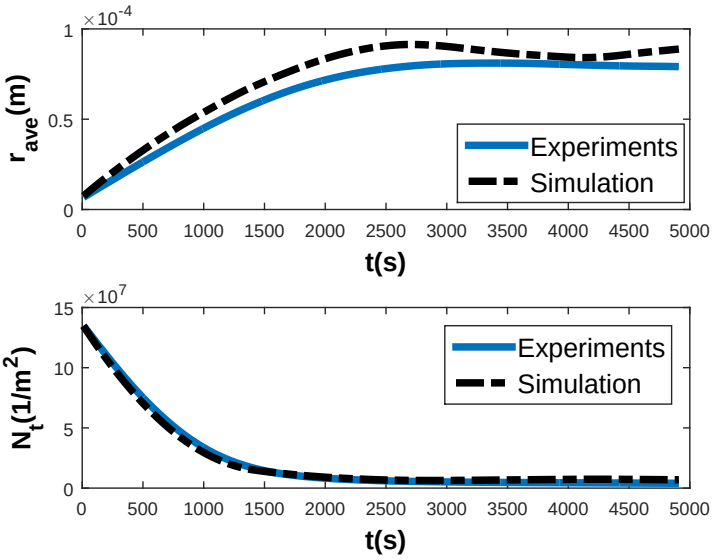

Figure 7: Changes in (a) droplet size and (b) droplets density during process time for simulation and experiments

on the surface. This indicates that there is no pair of droplets that can get closer than 6 μm unless they coalesce. The accordance between the graphs of experimental and simulation results indicates that the program could predict spatial distribution of droplets very well.

4.2 Effect of wall temperature

By calculating the average convection coefficient (h_{ave}) and total heat flux (q) from equations 6 and 7 at each step, we will be able to discuss the effect of T_w on the area occupied by droplets (ϕ) since these three parameters are related by:

$$\frac{q}{A} = h_{ave}\phi\Delta T_t, \tag{16}$$

In equation 16 A is the total area and $\phi = 100 \times \frac{A_{droplets}}{A}$, when $A_{droplets}$ is total area covered by droplets. h_{ave} depends strongly on the droplets size. According to figure 10 for small droplets near 10 μm, h_{ave} is near 300000 $W/m^2.K$ and it decreases to a constant value around 10000 $W/m^2.K$ for droplets bigger than 90 μm. This is why q during dropwise condensation is much higher than in filmwise condensation. When condensation occurs with small droplets, h_{ave} corresponds to very high values, by increasing droplets size, overall h_{ave} reduces and when droplets are big enough to wet the surface it goes down to less than one tenth of it's initial value.

r_{ave} is related to T_w by r_{min}. By increasing T_w (decreasing total temperature difference) r_{min} increases continuously. Generally, there are many sites that are potential to grow droplets of different sizes. By decreasing temperature difference between substrate and air saturated temperature, the driving force for nucleation of small droplets reduces and as a result small sites become inactive. In figure 11 it can be seen that the size of small active sites increased from 24 nm to near 34 nm by increasing T_w from 274K to 303K. By increasing r_{min}, the rate of adsorption decreases at earlier stages according to equation 9, but in the later stages r becomes bigger and bigger and the effect r_{min} becomes negligible. So T_w affects the size and number of small droplets in earlier stages but is not able to change these parameters for big droplets. Since h_{ave} is a function of both N_t and r_{ave}, changes in T_w will result in the same h_{ave} at later stages.

All in all it can be concluded that by increasing T_w, h_{ave} dose not change very significantly because although r_{min} increases, r_{ave} does not change in later stages. On the other hand, by

increasing T_w, the heat transfer driving force (ΔT_t) decreases, which will lead to a noticeable decrease in q. Both of these effects are presented in figure 12.

So according to equation 16, by decreasing ΔT_t, q decreases when h_{ave} is almost constant, which will result in almost constant pattern in the graph of ϕ too. Although in the earlier stages, in experiments with higher T_w the number of small nucleation sites with huge capacity of h_{ave} are lower than experiments with colder substrate, after a while the rate of adsorption and coalescence are the same for all T_w, which will result in the same ϕ between all the substrates. In figure 13 the changes in ϕ at different T_w is illustrated. As was said before, at the beginning small percentage of area is covered by liquid droplets but after a while coalescing drops start to cover substrate surface very rapidly. Continuing the process when coalescing drops become bigger, free area appears around them which reduces the rate of coalescence but is potential to grow new small droplets. After this step the fraction of area covered by water reaches it's stable value. These results are supported by experiments as is shown in figure 13. At first the initial droplets cover just around 2% of the substrate but after steady state ϕ reaches to near 70% for all T_w.

As was mentioned before, the main goal of this study is to increase illumination efficiency in car light shield by changing small dispersed droplets into big uniform ones. The graphs presented up to here indicate that by changing in T_w, ϕ does not change very significantly. The next parameter that is going to be discussed is N_D.

4.3 Effect of initial nucleation site density

In this section the results of simulation were examined for four different droplets densities of 4.9×10^7, 9.7×10^7, 1.29×10^8, $2.4 \times 10^8 m^{-2}$ in order to investigate the effect of this parameter on the regime change from dropwise to filmwise condensation.

Generally, when the process starts with denser substrate the rate of coalescence at first is higher, while the rate of adsorption is not different from substrates with lower densities. Droplets in denser substrate are closer together and can coalesce faster but after a while a vacant area appears around each droplet due to coalescence. In this free area new small droplets will nucleate rapidly, that will lower r_{ave} and increase N_t. This effect is indicated in figure 14 (a) and (b). According to these two plots, although in all of the numerical simulations the initial size of droplets are the same, by continuing the process surfaces with higher value of N_D are covered by smaller droplets at each step, but stay denser than the others during the whole process time. In the process with more initial droplets the rate of coalescence and production free area is higher, that will lead to lower ϕ at later stages. If one does not consider the effect of nucleation of new small droplets at each step, both of these graphs will show opposite results.

According to figure 15 although the amount of droplets at the beginning is different, at steady state the percentage of surface covered with water droplets is around 20% lower for substrate with $N_D = 2.4 \times 10^8 m^{-2}$ than substrate with $N_D = 4.9 \times 10^7 m^{-2}$. This difference also can give us the clue to study the droplets positioning on the surface besides N_D. Meaning that it is possible to increase ϕ by manipulating the position of droplets on the surface as well as their number. The arrangement of droplets on the surface will be studied by changing surface topography in the next step of our investigation.

5 Conclusion

A physical-based model was used to simulate spatial distribution of droplets in dropwise condensation. The main goal was to study the spatial distribution of droplets at each time step, and also to investigate the effect of T_w and N_D on the percentage of area occupied by the droplets. The predictions of the proposed model for the evolution of droplets size and droplets densities were in good agreement with experimental results. Also the spatial distribution estimated by model was the same as real droplets according to Ripley's L function at primary and steady state stages. It was shown that although T_w does not affect ϕ, N_D was able to decrease it. This bears in mind

the idea of controlling the rate of condensation by changing the arrangement of droplets on the surface and study remains open.

6 Acknowledgments

The authors are grateful to Rémi Berger and Elise Contraires, for their help in taking experimental results. This work was supported by the PSA-Openlab, LABEX MANUTECH-SISE (ANR-10-LABX-0075), within the program "Investissements d'Avenir" (ANR-11-IDEX-0007) operated by the French National Research Agency (ANR).

References

[1] E Schmidt, W Schurig, and W Sellschopp. Versuche über die kondensation von wasserdampf in film-und tropfenform. *Technische Mechanik und Thermodynamik*, 1(2):53–63, 1930.

[2] Xiuliang Liu and Ping Cheng. Lattice boltzmann simulation for dropwise condensation of vapor along vertical hydrophobic flat plates. *International Journal of Heat and Mass Transfer*, 64:1041–1052, 2013.

[3] Ching-Wen Lo, Chi-Chuan Wang, and Ming-Chang Lu. Spatial control of heterogeneous nucleation on the superhydrophobic nanowire array. *Advanced Functional Materials*, 24(9):1211–1217, 2014.

[4] Jorge R Lara and Mark T Holtzapple. Experimental investigation of dropwise condensation on hydrophobic heat exchangers. part ii: Effect of coatings and surface geometry. *Desalination*, 280(1):363–369, 2011.

[5] Leon R Glicksman and Andrew W Hunt. Numerical simulation of dropwise condensation. *International Journal of Heat and Mass Transfer*, 15(11):2251–2269, 1972.

[6] Earl E Gose, AN Mucciardi, and Eric Baer. Model for dropwise condensation on randomly distributed sites. *International Journal of Heat and Mass Transfer*, 10(1):15–22, 1967.

[7] BM Burnside and HA Hadi. Digital computer simulation of dropwise condensation from equilibrium droplet to detectable size. *International journal of heat and mass transfer*, 42(16):3137–3146, 1999.

[8] J.W. Rose E.J. Le Fevre. A theory of heat transfer by dropwise condensation. In *Proceedings of 3rd International Heat Transfer*, pages 362–375, 1966.

[9] JWf Rose. On the mechanism of dropwise condensation. *International Journal of Heat and Mass Transfer*, 10(6):755IN1757–756762, 1967.

[10] Hfroaki Tanaka. A theoretical study of dropwise condensation. *ASME J. Heat Transfer*, 97(1):72–78, 1975.

[11] Tsuruta Takaharu and Hiroaki Tanaka. A theoretical study on the constriction resistance in dropwise condensation. *International journal of heat and mass transfer*, 34(11):2779–2786, 1991.

[12] JW Rose and LR Glicksman. Dropwise condensation—the distribution of drop sizes. *International journal of heat and mass transfer*, 16(2):411–425, 1973.

[13] Maofei Mei, Feng Hu, Chong Han, and Yanhai Cheng. Time-averaged droplet size distribution in steady-state dropwise condensation. *International Journal of Heat and Mass Transfer*, 88:338–345, 2015.

[14] S Vemuri and KJ Kim. An experimental and theoretical study on the concept of dropwise condensation. *International journal of heat and mass transfer*, 49(3):649–657, 2006.

[15] Tianyi Song, Zhong Lan, Xuehu Ma, and Tao Bai. Molecular clustering physical model of steam condensation and the experimental study on the initial droplet size distribution. *International Journal of Thermal Sciences*, 48(12):2228–2236, 2009.

[16] MK El-Adawi and TH Felemban. Dropsize function during dropwise condensation in relation to heat transfer intensification—statistical approach. *Desalination and Water Treatment*, 24(1-3):244–250, 2010.

[17] Xiuliang Liu and Ping Cheng. Dropwise condensation theory revisited: Part i. droplet nucleation radius. *International Journal of Heat and Mass Transfer*, 83:833–841, 2015.

[18] Xiuliang Liu and Ping Cheng. Dropwise condensation theory revisited part ii. droplet nucleation density and condensation heat flux. *International Journal of Heat and Mass Transfer*, 83:842–849, 2015.

[19] SA Stylianou and JW Rose. Drop-to-filmwise condensation transition: heat transfer measurements for ethanediol. *International Journal of Heat and Mass Transfer*, 26(5):747–760, 1983.

[20] Paul Meakin. Droplet deposition growth and coalescence. *Reports on Progress in Physics*, 55(2):157, 1992.

[21] Xue-Hu Ma, Tian-Yi Song, Zhong Lan, and Tao Bai. Transient characteristics of initial droplet size distribution and effect of pressure on evolution of transient condensation on low thermal conductivity surface. *International Journal of Thermal Sciences*, 49(9):1517–1526, 2010.

[22] Paul Meakin. The structure of two-dimensional witten-sander aggregates. *Journal of Physics A: Mathematical and General*, 18(11):L661, 1985.

[23] JL McCormick and JW Westwater. Nucleation sites for dropwise condensation. *Chemical Engineering Science*, 20(12):1021–1036, 1965.

[24] AR Jameson and AB Kostinksi. What is a raindrop size distribution? *Bulletin of the American Meteorological Society*, 82(6):1169, 2001.

[25] Philip M Dixon. Ripley's k function. *Encyclopedia of environmetrics*, 3:1796–1803, 2002.

[26] Baojin Qi, Jinjia Wei, Li Zhang, and Hong Xu. A fractal dropwise condensation heat transfer model including the effects of contact angle and drop size distribution. *International Journal of Heat and Mass Transfer*, 83:259–272, 2015.

[27] Patricia B Weisensee, Yunbo Wang, Qian Hongliang, Daniel Schultz, William P King, and Nenad Miljkovic. Condensate droplet size distribution on lubricant-infused surfaces. *International Journal of Heat and Mass Transfer*, 109:187–199, 2017.

[28] P Meakin. Dropwise condensation: the deposition growth and coalescence of fluid droplets. *Physica Scripta*, 1992(T44):31, 1992.

[29] Michael Nosonovsky. Model for solid-liquid and solid-solid friction of rough surfaces with adhesion hysteresis. *The Journal of chemical physics*, 126(22):224701, 2007.

[30] Nenad Miljkovic, Ryan Enright, and Evelyn N Wang. Modeling and optimization of superhydrophobic condensation. *Journal of Heat Transfer*, 135(11):111004, 2013.

[31] Ichiro Tanasawa. Advances in condensation heat transfer. *Advances in heat transfer*, 21:55–139, 1991.

[32] JW Rose. Dropwise condensation theory. *International Journal of Heat and Mass Transfer*, 24(2):191–194, 1981.

[33] H Tanaka. Measurements of drop-size distributions during transient dropwise condensation. *Journal of Heat Transfer*, 97(3):341–346, 1975.

[34] Mousa Abu-Orabi. Modeling of heat transfer in dropwise condensation. *International journal of heat and mass transfer*, 41(1):81–87, 1998.

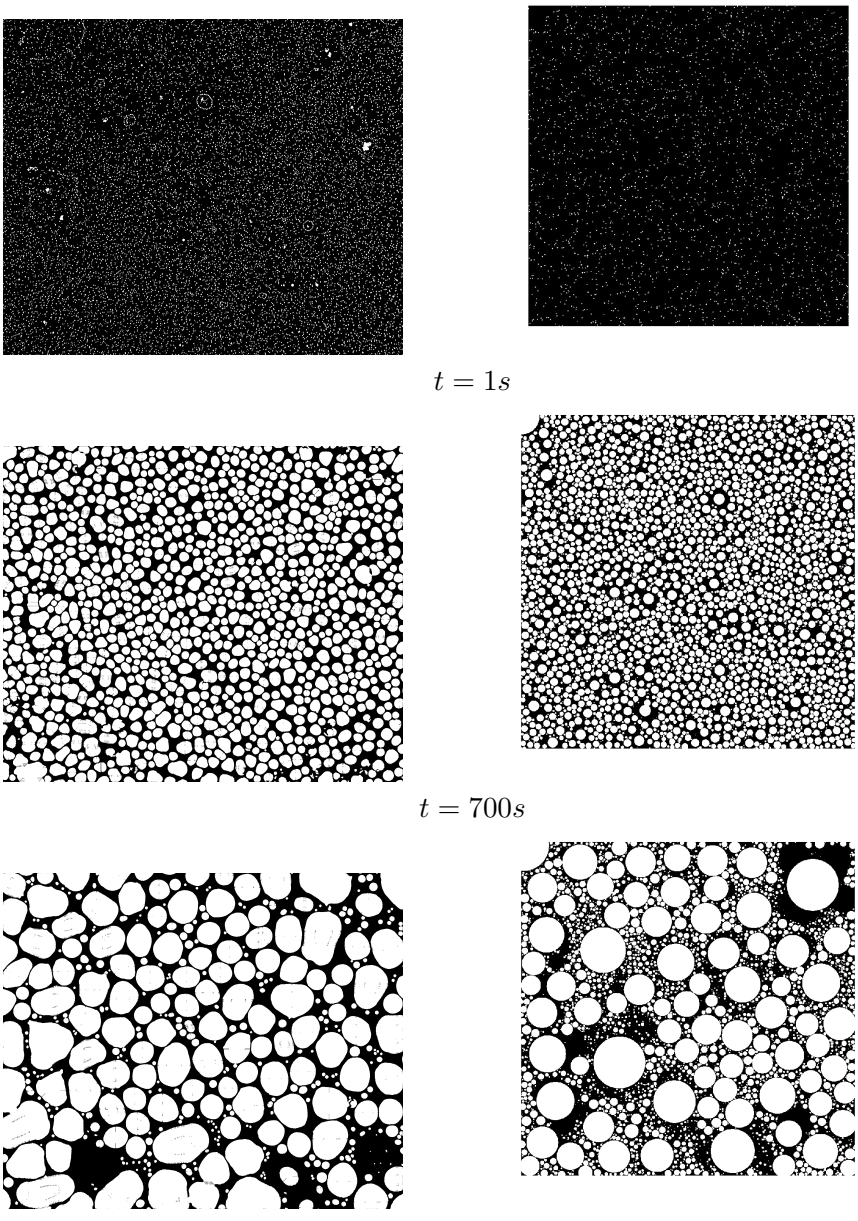

Figure 8: The growth of: (a) real droplets, and (b)droplets generated by proposed model at three different time intervals ($t = 1s$, $t = 700s$, $t = 5000s$).

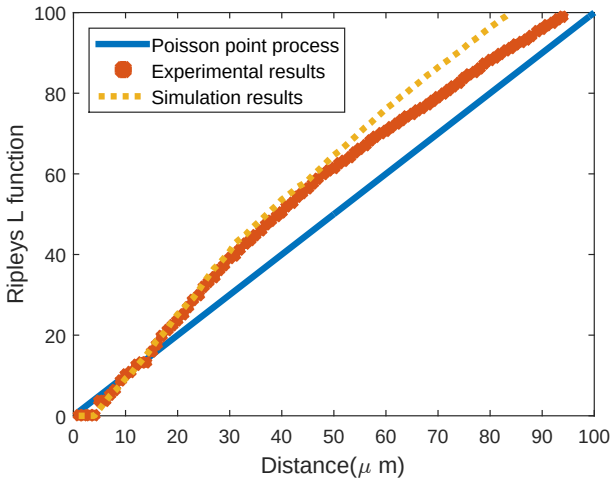

Figure 9: Comparison between Ripley's L functions of droplets at steady state relevant to the poisson point process, experiments and simulation

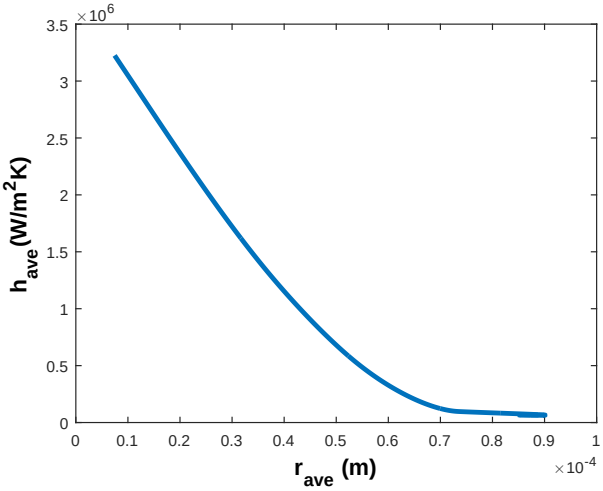

Figure 10: Average heat transfer coefficient $v.s$ average size of droplets

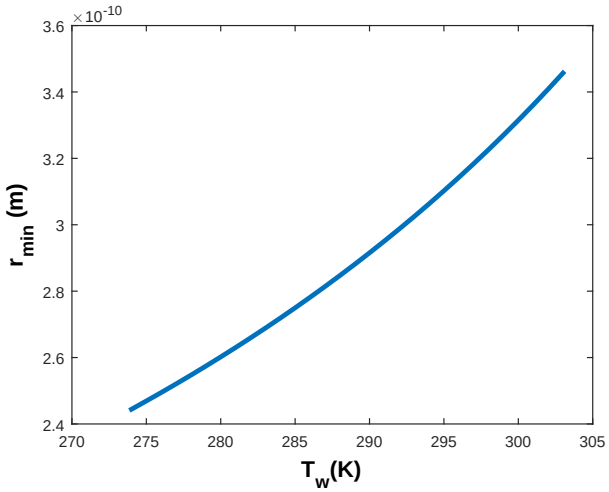

Figure 11: Minimum size of droplets that are able to grow $v.s$ wall temperature

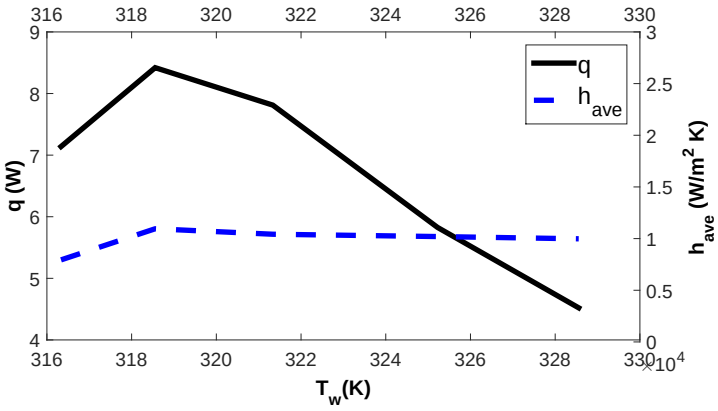

Figure 12: Evolution of Average heat transfer coefficient and total heat flux $v.s$ wall temperature

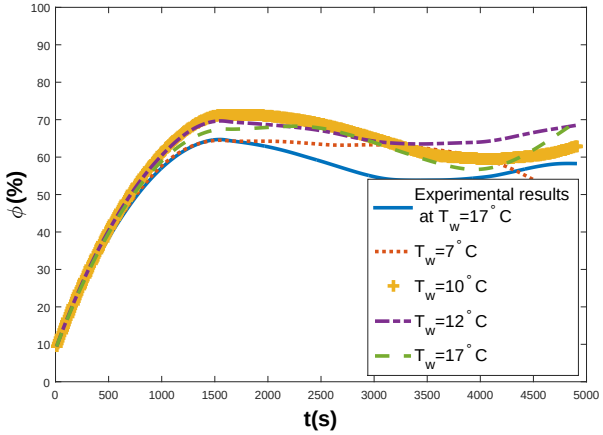

Figure 13: Percentage of surface coverage $v.s$ time

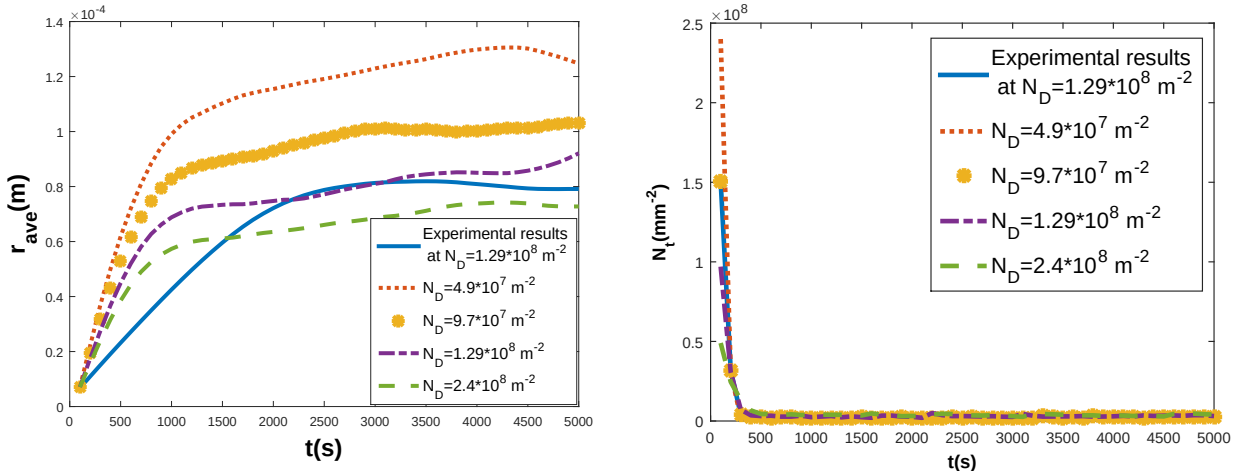

(a) (b)

Figure 14: (a) Droplets size and (b) droplets densities during progress time for different initial nucleation site densities

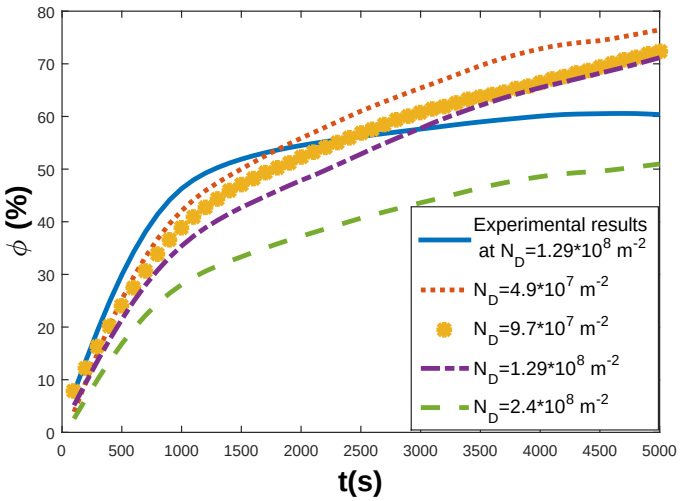

Figure 15: Surface coverage for different nucleation site densities $v.s$ time